2011 American Control Conference
on O'Farrell Street, San Francisco, CA, USA
June 29 - July 01, 2011

Path following for mechanical systems: Experiments and examples

Andre Hladio and Christopher Nielsen and David Wang

Abstract— **This paper concerns the design of path following controllers for mechanical systems. Our method is to find a coordinate and feedback transformation that puts the mechanical system in a convenient form for path following control design. In this form, linear and controllable subsystems govern motions toward and along the path. We choose a particular "virtual output" to perform input-output feedback linearization, and characterize when this virtual output can be used. We apply this technique to a planar five-bar linkage robot, and implement it experimentally, highlighting behaviour fundamentally different from standard tracking control. In simulation, we further illustrate our approach on an underactuated five-bar robot with a flexible link.**

I. Introduction

Machining [1], exercise and rehabilitation equipment, human-robot interaction [2] and obstacle avoidance [3] are examples where the specified output of a mechanical system must follow a prescribed path. For these types of applications, path following controllers, as opposed trajectory tracking controllers may be more appropriate. A trajectory tracking controller parameterizes the desired path using time and then eliminates the tracking error. Even if the output of the mechanical system lies on the path, but the tracking error is large, the feedback controller may drive the output off the path. This is clearly undesirable in, for instance, machining applications. This situation may arise due to unmodeled disturbances, improper initialization, or, when the reference trajectory is moving too quickly along the path. Alternatively, path following controllers do not rely on *a priori* parameterizations of the desired path and can ensure that, if the output is on the path, it remains on the path for all future time. In this paper we present experimental and simulation examples of an approach to designing path following controllers that builds on the approach in [4] and is applicable to a large class of mechanical systems.

Path following for general control systems has been studied elsewhere. In this paper, instead, we study path following for mechanical systems and briefly present relevant literature. *Path-constrained trajectory planning* was proposed to suitably "slow down" trajectories so that they are feasible for given robotic manipulators to follow [5]. *Contour following* is common in the control of machine tools, where the control objective is to closely follow a path [1]. In these approaches, ultimately time-parameterized trajectories must be implemented for control, meaning unmodeled disturbances and/or improper initialization may cause a departure from the path.

A. Hladio, C. Nielsen and D. Wang are with the Department of Electrical and Computer Engineering, University of Waterloo, Waterloo, ON, N2L 3G1, Canada. {ahladio, cnielsen, dwang}@uwaterloo.ca

An approach to designing path following controllers is to parameterize the desired path, then use the parameterization as a reference signal just as one would in trajectory tracking; however, the velocity of the reference point is treated as an extra control input, thus allowing the parameterization of the desired motion along the path be altered [6]. This method does not guarantee that the output stays on the path for all time. Conversely, the use of *virtual holonomic constraints* for path following does guarantee that the output stays on the path, as illustrated in an application to a forestry crane [7].

We treat path following as an instance of set stabilization. This approach is explored in [2], [4], [8]. We use the main results of [10], valid for general mechanical systems, to design path following controllers for robotic manipulators.

II. Path following control design

Given a mechanical system and a desired path defined in its output space, the control objective is to design a feedback controller that makes the output of the closed-loop system approach and traverse the path. Additionally we require output invariance of the path, i.e., if the system's output starts on the path with initial velocity tangent to it, then it remains on the path for all future time. Finally, given enough actuation, the controller must impose desired motion of the closed-loop mechanical system on the path itself.

The approach in [4], [9] ,is attractive for designing path following controllers because it guarantees output invariance of the path and because it decomposes the design process into two stages. In stage one we design a controller to make the output approach and stay on the path and in stage two we design a controller to achieve the desired motion on the path. The key difference between this work and previous work is that for mechanical systems it is possible to greatly simplify stage two, provided the system has sufficient actuation.

A. Class of systems

The Euler-Lagrange equations of an N degree-of-freedom (DOF) mechanical system are commonly written as

$$M(q)\ddot{q} + C(q,\dot{q})\dot{q} + G(q) = \tau, \tag{1}$$

where $q = \mathrm{col}\,(q_1, \ldots, q_N)$ are generalized configuration coordinates and $\tau \in \mathbb{R}^N$ is the vector of generalized forces, or inputs, acting on the system. For standard mechanical systems, under reasonable assumptions, the generalized mass matrix $M(q)$ is positive definite, and therefore invertible. In order to convert (1) into state space form and to distinguish between configuration and velocity states, let $x_c := q$, $x_v := \dot{q}$, and $x := (x_c, x_v) = \mathrm{col}\,(x_{c_1}, \ldots x_{c_N}, x_{v_1}, \ldots, x_{v_N}) = \mathrm{col}\,(q_1, \ldots, q_N, \dot{q}_1, \ldots \dot{q}_N)$. Define $n := 2N$ and treat the

978-1-4577-0079-8/11/$26.00 ©2011 AACC

state x as an element of $\mathbb{R}^n$. We do not yet make any assumptions about the degree of actuation of the mechanical system. Hence τ has $0 \leq m \leq N$ independent applied forces. Define $g_v(x_c)u := M^{-1}(x_c)\tau$, where $g_v(x_c) \in \mathbb{R}^{N\times m}$ and $u \in \mathbb{R}^m$. Finally, set $f_v(x) := -M^{-1}(x_c)C(x_c, x_v)x_v - M^{-1}(x_c)G(x_c)$, where $f_v(x) \in \mathbb{R}^{N\times 1}$. With these definitions, the equations of motion in state space form are

$$\dot{x} = f(x) + g(x)u := \begin{bmatrix} x_v \\ f_v(x) \end{bmatrix} + \begin{bmatrix} 0_{N\times m} \\ g_v(x_c) \end{bmatrix} u, \qquad (2)$$

where $f : \mathbb{R}^n \to \mathbb{R}^n$ and $g : \mathbb{R}^n \to \mathbb{R}^{n\times m}$ are assumed to be smooth. The output of (2) is the variable we are interested in controlling. We restrict the class of output functions to solely be smooth functions of the configuration variables

$$y = h(x), \quad \frac{\partial h(x)}{\partial x_v} = 0, \quad y \in \mathbb{R}^p. \qquad (3)$$

B. Path assumptions

The control objective is to have the output (3) of (2) follow a smooth parameterized curve, $\sigma : \mathbb{D} \to \mathbb{R}^p$, where $\mathbb{D}$ is either $\mathbb{R}$ when the curve is not closed or $\mathbb{D} = \mathbb{S}^1$ when the curve is closed[1].

Assumption 1: The path, $\sigma(\mathbb{D})$, is an embedded submanifold of $\mathbb{R}^p$ with dimension 1.

Assumption 2: There exists a smooth map $s : \mathbb{R}^p \to \mathbb{R}^{p-1}$ such that 0 is a regular value of s and $\sigma(\mathbb{D}) = s^{-1}(0)$. Let $\gamma := s^{-1}(0)$. Moreover the *lift* of γ to $\mathbb{R}^n$

$$\Gamma := (s \circ h)^{-1}(0) = \{x \in \mathbb{R}^n : s(h(x)) = 0\}$$

is a submanifold of $\mathbb{R}^n$.

The path following manifold, denoted $\Gamma^\star$, with dimension $n^\star$, associated with the curve γ is the maximal controlled invariant subset of Γ. Physically it consists of all those motions of the mechanical system (2) for which the output (3) can be made to remain on the curve γ by suitable choice of control signal [4]. The existence of $\Gamma^\star$ is assured as long as the path γ is a feasible path for the mechanical system.

C. Desired normal form

If the function $\lambda(x)$ yields a well-defined relative degree at some point on $\Gamma^\star$ then we can perform input-output feedback linearization for non-square systems at that point. If this holds at some $x^\star \in \Gamma^\star$, then there exists a coordinate transformation $T : x \mapsto (\eta, \xi)$, defined in a neighbourhood U of $x^\star$, and feedback transformation $u = \alpha(x) + \beta(x)v$ such that $T(\Gamma^\star \cap U) = \{(\eta, \xi) : \xi = 0\}$ and in (η, ξ) coordinates system (2) reads

$$\begin{aligned} \dot{\eta} &= f^0(\eta, \xi) + g^\pitchfork(\eta, \xi)v^\pitchfork + g^\parallel(\eta, \xi)v^\parallel \\ \dot{\xi} &= A\xi + Bv^\pitchfork \end{aligned} \qquad (4)$$

with $v = \mathrm{col}\,(v^\pitchfork, v^\parallel) \in \mathbb{R}^m$ and (A, B) a controllable pair.

The utility of the normal form (4) for path following comes from the decomposition of the dynamics into η and ξ subsystems, and the control into two groups, $v^\parallel$ and $v^\pitchfork$. The ξ subsystem describes the motion off the set $\Gamma^\star$. We call these the transversal dynamics. If one can ensure no finite escape times, then $v^\pitchfork$ can be used to stabilize $T(\Gamma^\star \cap U)$. If the trajectories of the closed-loop system are bounded, then the stabilization of $T(\Gamma^\star \cap U)$ implies that of $\Gamma^\star \cap U$, and therefore making the path attractive in output space. This controller also ensures output invariance of the path because the origin of the ξ subsystem is an equilibrium point.

Once on the set, the system dynamics reduce to $\dot{\eta} = f^0(\eta, 0) + g^\parallel(\eta, 0)v^\parallel$. We call these the tangential dynamics. In general, designing $v^\parallel$ to achieve desired motion along the path may be difficult or impossible because the tangential dynamics have very little structure. For mechanical systems with sufficient actuation it is possible to impose further structure on the tangential dynamics that greatly simplifies the design of $v^\parallel$ to achieve desired motion on the path.

To this end, we seek a coordinate and feedback transformation that refines (4) and puts the η dynamics in the form

$$\begin{aligned} \dot{\eta}_1 &= f^0(\eta, \xi) + g^\pitchfork(\eta, \xi)v^\pitchfork + g_1^\parallel(\eta, \xi)v_1^\parallel + g_2^\parallel(\eta, \xi)v_2^\parallel \\ \dot{\eta}_2 &= A^\parallel\eta_2 + B^\parallel v_2^\parallel \end{aligned} \qquad (5)$$

where $\eta := (\eta_1, \eta_2)$, $\dim(\eta_1) = n^\star - 2$, $\dim(\eta_2) = 2$, $(A^\parallel, B^\parallel)$ is controllable, and $v^\parallel = (v_1^\parallel, v_2^\parallel)$. We also require that for all $\tilde{x}, \hat{x} \in \mathbb{R}^n$

$$h(\tilde{x}) \neq h(\hat{x}) \text{ and } h(\hat{x}), h(\tilde{x}) \in \gamma \Rightarrow \eta_2(\tilde{x}) \neq \eta_2(\hat{x}). \qquad (6)$$

To understand the physical intuition behind the dynamics (5) and why they are useful for designing path following controllers, suppose that $\xi = 0$, i.e., the system is on the path following manifold. The tangential dynamics become

$$\begin{aligned} \dot{\eta}_1 &= f^0(\eta, 0) + g_1^\parallel(\eta, 0)v_1^\parallel + g_2^\parallel(\eta, 0)v_2^\parallel \\ \dot{\eta}_2 &= A^\parallel\eta_2 + B^\parallel v_2^\parallel. \end{aligned}$$

At any two points on the path following manifold, $(\tilde{\eta}_1, \tilde{\eta}_2)$ and $(\hat{\eta}_1, \hat{\eta}_2)$, the output (3) of system (2) lies on the desired path γ. However, if $\tilde{\eta}_2 \neq \hat{\eta}_2$ then the output is on different points on the path. Hence the η_2 subsystem determines where on the path the system output lies, and since $(A^\parallel, B^\parallel)$ is controllable, we can use $v_2^\parallel$ to completely determine the motion along the curve. On the other hand, the η_1 subsystem, which is nonlinear in general, represents the dynamics on the path following manifold that do not produce observable motion along the path in the output space. Uncontrollable tangential dynamics also appear in the η_1 dynamics.

D. Coordinate and feedback transformation

In order to impose additional structure on the tangential dynamics, we will use input-output feedback linearization, choosing the output to be a particularly useful function for path following. Denote the tubular neighbourhood of γ as $\gamma_\epsilon \subset \mathbb{R}^p$. Define a projection operator that maps the output $y \in \gamma_\epsilon$ to a unique point $\theta \in \mathbb{D}$ such that the point $\sigma(\theta) \in \gamma$

[1]The notation $\mathbb{S}$ means $\mathbb{R} \bmod 2\pi$, the real numbers modulo 2π. On the set $\mathbb{S}^1$ two different real numbers x and $x + 2\pi$ are considered to be the same point. Thus $\mathbb{S}^1$ has the geometric structure of a circle.

is closest to y,

$$\begin{aligned} \varpi :&\gamma_\epsilon \to \mathbb{D} \\ &\varpi(y) = \arg\min_{\theta\in\mathbb{D}} \|y - \sigma(\theta)\|. \end{aligned} \tag{7}$$

Intuitively, this describes the "distance" of the output along the path. Composing this projection with the output of the mechanical system, we obtain a function $\pi : \mathbb{R}^n \to \mathbb{D}$, $\pi(x) = \varpi \circ h(x)$. Next consider the function

$$\begin{aligned} \lambda :&\mathbb{R}^n \to \mathbb{R}^{p-1} \\ &\lambda(x) = s \circ h(x). \end{aligned} \tag{8}$$

This function locally describes the "distance" to the path following manifold. We use the functions (7) and (8) to generate a virtual output

$$\hat{y} = \begin{bmatrix} \pi(x) \\ \lambda(x) \end{bmatrix} = \begin{bmatrix} \varpi \circ h(x) \\ s \circ h(x) \end{bmatrix}. \tag{9}$$

If this output yields a well-defined relative degree at some point on $\Gamma^\star$ then system (2) is locally feedback equivalent to the desired normal form

$$\begin{aligned} \dot{\eta}_1 &= f^0(\eta,\xi) + g^\pitchfork(\eta,\xi)v^\pitchfork + g_1^\parallel(\eta,\xi)v_1^\parallel + g_2^\parallel(\eta,\xi)v_2^\parallel \\ \dot{\eta}_2 &= A^\parallel\eta_2 + B^\parallel v_2^\parallel \\ \dot{\xi} &= A\xi + Bv^\pitchfork. \end{aligned} \tag{10}$$

The next result characterizes whether or not (9) yields a well-defined relative degree.

Theorem 2.1: Given a mechanical control system (2) and a path γ in output space satisfying Assumptions 1 and 2, let $x^\star = (x_c^\star, x_v^\star) \in \mathbb{R}^n$ satisfy $h(x^\star) \in \gamma$. The system (2) with output (9) yields a well-defined vector relative degree of $\{2,\dots,2\}$ at $x^\star = (x_c^\star, x_v^\star)$ if and only if

$$\dim\left(\mathrm{Im}\left(\left.\frac{\partial h}{\partial x_c}\right|_{x_c=x_c^\star} g_v(x_c^\star)\right)\right) = p. \tag{11}$$

holds at $x^\star$.

III. Planar five-bar robot path following

We apply the approach to designing path following controllers described in Section II to an experimental platform consisting of a 2-DOF five-bar linkage robot with rigid links [11]. This robot is mechanically designed such that it is linear and time-invariant.

A. Model

The planar five-bar linkage robot is illustrated in Figure 1. The full derivation of this model is well documented [11], and therefore omitted. This fully-actuated robot is mechanically designed to be dynamically decoupled and gravity balanced [11, Section 6.4.1], so that the Euler-Lagrange equations for this system are

$$\begin{aligned} M_{11}\ddot{q}_1 + b_1\dot{q}_1 &= \tau_1 \\ M_{22}\ddot{q}_2 + b_2\dot{q}_2 &= \tau_2, \end{aligned} \tag{12}$$

where $M_{11}, M_{22}, b_1, b_2 > 0$ are constants, and $\tau := \mathrm{col}\,(\tau_1,\tau_2)$ is a vector of applied motor torques. Let $x_c = \mathrm{col}(x_{c_1}, x_{c_2}) := \mathrm{col}(q_1,q_2)$ and $x_v = \mathrm{col}(x_{v_1}, x_{v_2}) := \mathrm{col}(\dot{q}_1,\dot{q}_2)$, and set $u := \tau$ for consistency with notation in (2). The system (12) may be expressed in the form (2) as $\dot{x} = Fx + Gu$. Let the output, $y \in \mathbb{R}^2$, of (12) denote the position of the end-point of the robot

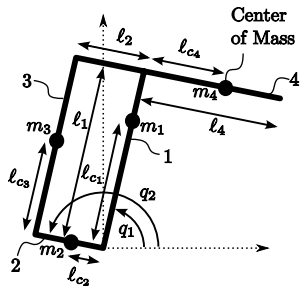

Fig. 1. Two degree-of-freedom five-bar linkage robot.

$$y = h(x) := \begin{bmatrix} \ell_1\cos x_{c_1} - \ell_4\cos x_{c_2} - \ell_4 \\ \ell_1\sin x_{c_1} - \ell_4\sin x_{c_2} - \ell_1 \end{bmatrix}. \tag{13}$$

B. Path following

For the 2-DOF five-bar manipulator (12) with output (13), we check condition (11) of Theorem 2.1. The matrix $\frac{\partial h}{\partial x_c} g_v(x_c)$ is non-singular, and therefore has rank $p = 2$, if and only if the configuration corresponding to

$$x_{c_1} - x_{c_2} = k\pi,\ k \in \mathbb{Z} \tag{14}$$

is avoided. Condition (14) corresponds to where the parallelogram in Figure 1 collapses and all the links are collinear; the path must be chosen to avoid such configurations.

To illustrate this we choose a circular path of radius r, centered at the origin of the output space, given by $\sigma(\theta) = \mathrm{col}\,(r\cos\theta,\ r\sin\theta)$. The circular path may be written as

$$\gamma := \left\{(y_1,y_2) \in \mathbb{R}^2 : s(y) := y_1^2 + y_2^2 - r^2 = 0\right\}. \tag{15}$$

To put this system into the normal form (10) we will perform input-output feedback linearization using the virtual output (9). The function $\pi(x)$ is chosen as $\pi(x) = \varpi \circ h(x_c)$ where $\varpi(y) = \arg\min_{\theta\in[0,2\pi)} \|y - \sigma(\theta)\|$ is the projection of the output onto the path. In the case of a circle, we may use the angle of the output along the path, i.e., $\varpi(y) = \arg(y_1 + iy_2)$. The function $\lambda(x) = s \circ h(x)$ is obtained from (13) and (15). By Theorem 2.1, the virtual output $\hat{y} = \mathrm{col}(\pi(x), \lambda(x))$ yields a well-defined relative degree of $\{2,2\}$ at any point of the path as long as the condition (14) is avoided, i.e., when the circle lies in the robot's workspace.

The desired normal form can be obtained by letting $\xi := \mathrm{col}\,(\lambda(x), L_{Fx}\lambda(x))$ and $\eta := \mathrm{col}\,(\pi(x), L_{Fx}\pi(x))$. In (η,ξ)-coordinates the system takes the form

$$\begin{aligned} \dot{\eta}_2^1 &= \eta_2^2 \\ \dot{\eta}_2^2 &= L_{Fx}^2\pi(x)|_{x=T^{-1}(\eta,\xi)} + L_G L_{Fx}\pi(x)|_{x=T^{-1}(\eta,\xi)} u \\ \dot{\xi}_1 &= \xi_2 \\ \dot{\xi}_2 &= L_{Fx}^2\lambda(x)|_{x=T^{-1}(\eta,\xi)} + L_G L_{Fx}\lambda(x)|_{x=T^{-1}(\eta,\xi)} u. \end{aligned}$$

By Theorem 2.1, (9) yields a well defined relative degree and we take

$$\begin{bmatrix} u_1 \\ u_2 \end{bmatrix} = \begin{bmatrix} L_G L_{Fx}\pi(x) \\ L_G L_{Fx}\lambda(x) \end{bmatrix}^{-1}_{x=T^{-1}(\eta,\xi)} \left(\begin{bmatrix} -L^2_{Fx}\pi(x) \\ -L^2_{Fx}\lambda(x) \end{bmatrix}^{-1}_{x=T^{-1}(\eta,\xi)} + \begin{bmatrix} v_2^{\parallel} \\ v^{\pitchfork} \end{bmatrix} \right) \tag{16}$$

as our feedback transformation where $(v_2^{\parallel}, v^{\pitchfork}) \in \mathbb{R}^2$ are new control inputs. The closed-loop system in (η_2, ξ)-coordinates after the feedback (16) has the form

$$\begin{aligned} \dot{\eta}_2^1 &= \eta_2^2 \\ \dot{\eta}_2^2 &= v_2^{\parallel} \\ \dot{\xi}_1 &= \xi_2 \\ \dot{\xi}_2 &= v^{\pitchfork}. \end{aligned} \tag{17}$$

1) Control design: We stabilize the origin of the transversal subsystem in (17) by means of a PID compensator,

$$v^{\pitchfork}(\xi) = -K_1\xi_1 - K_2\xi_2 - K_3 \int_0^t \xi_1(\tau)d\tau, \tag{18}$$

with positive gains K_i, $i \in \mathbf{3}$. Since $v^{\pitchfork}(0) = 0$, $\xi = 0$ is an equilibrium point of the closed-loop transversal subsystem, $\Gamma^\star$ is controlled invariant. This ensures output invariance of the path as required.

Achieving the desired motion along the path is equivalent to making sure that either the angular velocity $\eta_2^2(t)$ approaches a desired reference profile $\eta_2^{2\text{ref}}(t)$ or that η_2^1 approach a desired position $\eta_2^{1\text{ref}} \in \mathbb{S}^1$. These goals can be achieved using the tangential control input by means of a simple proportional feedback with feedforward action

$$v^{\parallel} = -K_4\left(\eta_2^1 - \eta_2^{1\text{ref}}\right) + \dot{\eta}_2^{2\text{ref}}(t) - K_5\left(\eta_2^2 - \eta_2^{2\text{ref}}(t)\right). \tag{19}$$

2) Experimental setup: The experimental platform includes a gravity balanced and dynamically decoupled five-bar robot fabricated at the University of Waterloo [12], actuated by direct drive DC motors with optical encoders.

3) System identification: The model parameters b_1, b_2, M_{11} and M_{22} of (12), were found using the system identification procedure in [12], and are presented in [15, Table 4.1].

4) Experimental Results: Two experiments are considered to test the proposed path following control strategy with a circular path γ of radius 0.05 m.

Experiment 1: In the first experiment we make $y \to \gamma$ and simultaneously stabilize a particular position $\eta_2^{1\text{ref}} = \frac{\pi}{2}$ on γ. Figure 2 shows the robot end-point position and the circle γ in output space. Note that the end-point does not cut across the circle in order to reach the desired position, but follows the circular path. Figure 3 plots ξ, η and u versus time.

Experiment 2: This experiment demonstrates one of the key advantages of path following over trajectory tracking. Here the five-bar linkage robot end-point tracks a desired constant velocity profile, i.e., $\eta_2^{2\text{ref}} = 2\pi$ rad/s. We then temporarily constrain the end-point from moving in the tangential direction of traversal by physically obstructing the path. The end-point is free to move in any other direction. The results shown in Figure 5 clearly demonstrate an important feature of path following control, as the end-point remains on the path throughout. Tracking of the desired velocity profile resumes after the obstruction is removed without ever deviating from the path.

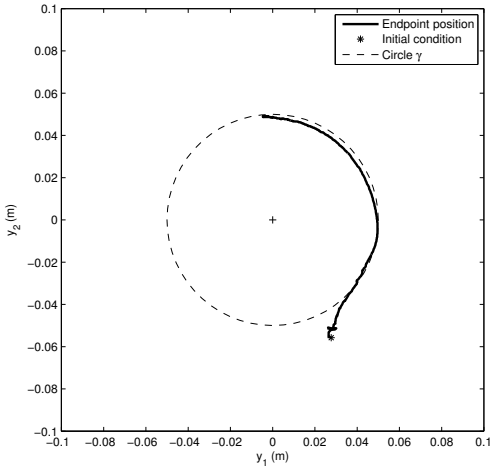

Fig. 2. End-point trajectory in output space for stabilizing desired position on the circle

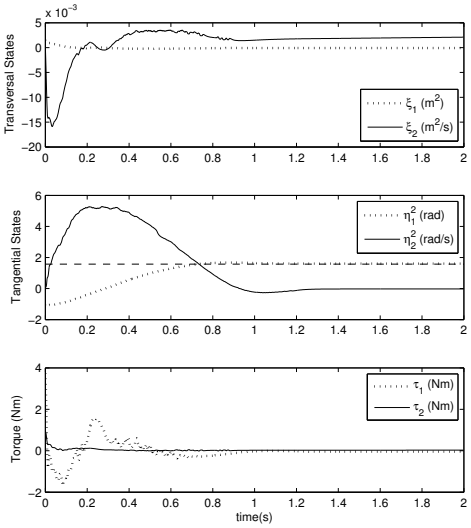

Fig. 3. Transformed states and control effort for end-point position control

IV. Flexible robot path following

The second example of a mechanical system we consider in this paper is a five-bar robot with output $y \in \mathbb{R}^3$, whose last link is flexible.

A. Model

We consider the flexible five-bar manipulator, shown in Figure 4, whose model is found in [13]. Its last link is a beam of length ℓ, flexible in the horizontal direction. We use the classic Euler-Bernoulli [14] model, which is approximated

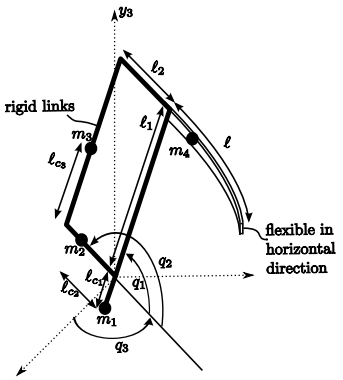

Fig. 4. A five-bar manipulator with horizontal flexibility in the last link

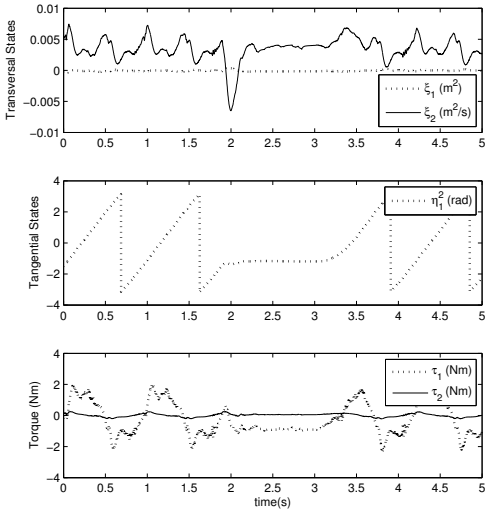

Fig. 5. Demonstration of path following control by showing transformed states and control effort with temporarily obstructed output

as a set of ODE's using the assumed modes approach with clamped free boundary conditions. The model is simplified by gravity-balancing, dynamic decoupling, and a preliminary feedback cancellation as in [13]. Our overall model may be written in the form (2) where

$$f_v(x) = \begin{bmatrix} 0 \\ 0 \\ \frac{1}{M'} \sum_{j=4}^{N} \Psi_j(x_c)\Omega_j(x) \\ \frac{-\rho}{M'}\Psi_4(x_c) \sum_{j=4}^{N} \Psi_j(x_c)\Omega_j(x) - \frac{\Omega_4(x)}{\rho} \\ \vdots \\ \frac{-\rho}{M'}\Psi_N(x_c) \sum_{j=4}^{N} \Psi_j(x_c)\Omega_j(x) - \frac{\Omega_N(x)}{\rho} \end{bmatrix} \tag{20}$$

and

$$g_v(x_c)u = \begin{bmatrix} \frac{1}{M_{11}} & 0 & 0 \\ 0 & \frac{1}{M_{22}} & 0 \\ 0 & 0 & \frac{1}{M'} \\ 0 & 0 & \frac{-\rho}{M'}\Psi_4(x_c) \\ 0 & 0 & \frac{-\rho}{M'}\Psi_5(x_c) \\ \vdots & \vdots & \vdots \\ 0 & 0 & \frac{-\rho}{M'}\Psi_N(x_c) \end{bmatrix} \begin{bmatrix} u_1 \\ u_2 \\ u_3 \end{bmatrix}. \tag{21}$$

The expressions for the smooth, nonlinear, scalar-valued functions $\Psi_j(x_c), \Omega_j(x)$, and $M'(x_c)$ are found in [15].

We are interested in controlling the position of the tip of the flexible link on the five-bar manipulator. Therefore, as the output, we choose the Cartesian position of the flexible link tip in the output space, $y = h(x)$, where

$$h(x) := \begin{bmatrix} (\ell_1 \cos x_{c_1} - \ell \cos x_{c_2}) \cos x_{c_3} - w(x_c) \sin x_{c_3} \\ (\ell_1 \cos x_{c_1} - \ell \cos x_{c_2}) \sin x_{c_3} + w(x_c) \cos x_{c_3} \\ \ell_1 \sin x_{c_1} - \ell \sin x_{c_2} - \ell_1 \end{bmatrix} \tag{22}$$

is an approximation valid for small deflections [13]. The model parameters chosen are found in [15].

B. Application of path following

For the flexible five-bar manipulator with structure (2), with (20), (21) and (22), we check condition (11) of Theorem 2.1. The determinant of $\frac{\partial h}{\partial x_c} g_v(x_c)$ is zero when the parallelogram making up the five-bar linkage robot collapses, or when the output is in particular regions very near the extremities of the workspace (see Figure 5.8 in [15]), and are easily avoidable. Avoiding these configurations, a path following controller may be designed using the approach of Section II for any path satisfying Assumptions 1 and 2.

We choose an ellipse as the path expressed as $\gamma := \{y \in \mathbb{R}^3 : s(y) = 0\}$, where

$$s(y) = \begin{bmatrix} y_2^2 + (y_3 - \ell_1)^2 - r^2 \\ y_1 - b y_2 - d \end{bmatrix} \tag{23}$$

and $r = 0.05$m, $b = 0.1$, $d = 0.5$m. As discussed in Section II, we choose the virtual output (9) using $\lambda(x) = s \circ h(x)$, and $\pi(x) = \varpi \circ h(x)$, where the projection $\varpi(y) = \arg\min_{\theta \in [0, 2\pi)} \|y - \sigma(\theta)\|$, describes the angular position of the output with respect to the path, i.e., $\varpi(y) = \arg(y_2 + (y_3 - \ell_1)i)$.

By Theorem 2.1, if the unacceptable configurations are avoided, then the virtual output yields a well-defined relative degree. Using this output and performing input-output feedback linearization we obtain the desired normal form (10) with $\xi \in \mathbb{R}^4$, $\eta_2 = \text{col}(\eta_2^1, \eta_2^2) \in \mathbb{R}^2$, $\eta_1 \in \mathbb{R}^6$. The ξ dynamics govern output motions transverse to the path, the η_2 dynamics govern output motions along the path, and the η_1 dynamics govern motions which are "tangential", but do not cause observable output motions (i.e., the internal, uncontrollable vibrations of the robot).

C. Simulation

We use a PID compensator to stabilize the origin of the ξ-subsystem. To control the tangential motions, we use the control law $v_2^{\parallel} = -5\left(\eta_2^2 - \eta_2^{2\text{ref}}\right)$, where

$$\eta_2^{2\text{ref}} = \begin{cases} 2 \text{ rad/s} & 0 \leq t < 3\text{s} \\ -2 \text{ rad/s} & t \geq 3\text{s}. \end{cases}$$

Figure 6 shows the Cartesian position of the flexible tip in output space, with the transformed states in In Figure 7.

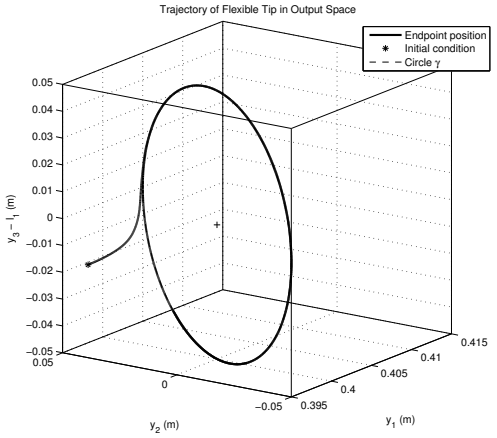

Fig. 6. Flexible tip in output space - tracking speed profile

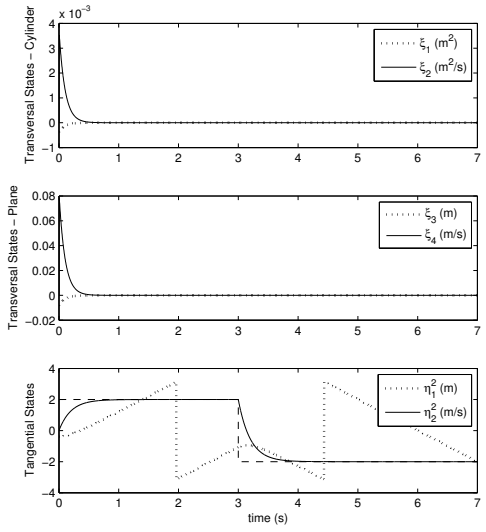

Fig. 7. Simulated transversal and tangential states

V. Discussion

We present a control design method to meet the path following control objective for mechanical systems. A coordinate and feedback transformation are used to put to the system in a form where linear controllers are used to meet the objective. Determining whether such a decomposition is possible involves checking the rank of a matrix.

This technique was experimentally implemented on a planar five-bar robot, with distinct advantages over trajectory tracking highlighted in *Experiment 2*. Simulation illustrates our approach applied to an underactuated and non-minimum phase system, where standard feedback linearization fails [13]. Furthermore, using a fictitious output is a common modeling technique used to simplify control of flexible beams, for instance, the reflected tip position is used in [16]. Although deflections are assumed small, it is desirable to control the actual tip position, as in our approach, rather than the position of a fictitious output.

References

[1] G.-C. Chiu and M. Tomizuka, "Contouring control of machine tool feed drive systems: a task coordinate frame approach," *Control Systems Technology, IEEE Transactions on*, vol. 9, no. 1, pp. 130 –139, Jan. 2001.

[2] P. Li and R. Horowitz, "Passive velocity field control of mechanical manipulators," *Robotics and Automation, IEEE Transactions on*, vol. 15, no. 4, pp. 751 –763, Aug. 1999.

[3] T. Tarn, N. Xi, and A. Bejczy, "Path-based approach to integrated planning and control for robotic systems," *Automatica*, vol. 32, no. 12, pp. 1675–1687, 1996.

[4] C. Nielsen, C. Fulford, and M. Maggiore, "Path following using transverse feedback linearization: Application to a maglev positioning system," *Automatica*, vol. 46, no. 3, pp. 585–590, 2010.

[5] S. M. LaValle, *Path Planning*. New York: Cambridge University Press, 2006.

[6] R. Skjente, T. Fossen, and P. Kokotović, "Robust output maneuvering for a class of nonlinear systems." *Automatica*, vol. 40, no. 3, pp. 373–383, March 2004.

[7] U. Mettin, P. X. La Hera, D. O. Morales, A. S. Shiriaev, L. B. Freidovich, and S. Westerberg, "Path-constrained trajectory planning and time-independent motion control: Application to a forestry crane," in *14th International Conference on Advanced Robotics (ICAR), Proceedings*, 2009.

[8] A. Shiriaev, J. Perram, and C. Canudas-de Wit, "Constructive tool for orbital stabilization of underactuated nonlinear systems: Virtual constraints approach," *Automatic Control, IEEE Transactions on*, vol. 50, no. 8, pp. 1164 – 1176, Aug. 2005.

[9] C. Nielsen and M. Maggiore, "On local transverse feedback linearization," *SIAM Journal on Control and Optimization*, vol. 47, no. 5, pp. 2227–2250, 2008.

[10] A. Hladio, C. Nielsen, and D. Wang, "Path following controller design for a class of mechanical systems," in *18th IFAC World Congress*, Milan, Italy, 2011, accepted.

[11] M. W. Spong and M. Vidyasagar, *Robot Dynamics and Control*. John Wiley and Sons, 1989.

[12] D. R. Madill, "Modelling and Control of a Haptic Interface: A Mechatronics Approach," Ph.D. dissertation, University of Waterloo, 1998.

[13] D. Wang and M. Vidyasagar, "Control of a class of manipulators with a single flexible link: Part 1 feedback linearization," *Journal of Dynamic Systems, Measurement and Control*, vol. 113, pp. 655–662, 1991.

[14] R. H. Cannon and E. Schmitz, "Initial Experiments on the End-Point Control of a Flexible One-Link Robot," *International Journal on Robotics Research*, vol. 3, no. 3, pp. 62–75, 1984.

[15] A. Hladio, "Path following for mechanical systems applied to robotic manipulators," Master's thesis, University of Waterloo, 2010.

[16] D. Wang and M. Vidyasagar, "Transfer functions for a single flexible link," *International Journal of Robotics Research*, vol. 10, no. 5, 1991.